

Experimental Investigation on the Effect of Diaphragm Flexibility on Out-of-Plane Dynamic Stability of Unreinforced Masonry Walls

O. Penner & K.J. Elwood

University of British Columbia, Canada



15 WCEE
LISBOA 2012

SUMMARY:

The vulnerability of unreinforced masonry (URM) buildings to out-of-plane damage and collapse has been clearly demonstrated in past earthquakes, most recently in the 2010 and 2011 earthquakes near Christchurch, New Zealand. This paper describes an experimental study examining the out-of-plane stability under seismic loading of URM walls connected to flexible diaphragms. Full-scale unreinforced solid clay brick wall specimens spanning one storey were subjected to earthquake ground motions on a shaking table. The top and bottom of the walls were connected to the shaking table through coil springs, simulating the effect of flexible diaphragms. The apparatus allowed the wall supports to undergo large absolute displacements, as well as out-of-phase top and bottom displacements, consistent with the expected performance of URM buildings with unretrofitted timber diaphragms. Three wall specimens were tested; the boundary conditions and wall dimensions were varied between specimens. Experimental results are compared with current assessment guidelines.

Keywords: Unreinforced Masonry; Out-of-Plane; Shaking Table; Diaphragm; Wall

1. INTRODUCTION

Buildings with unreinforced masonry (URM) walls have experienced considerable damage in past earthquakes. The typical damages that URM buildings suffer include: collapse of parapets or gables, diagonal shear failure or sliding shear failure of in-plane walls, and out-of-plane failure. Of these failure modes, out-of-plane wall failures pose the greatest risk to the safety of the people inside and outside of the building, since this mode will result in collapse of the load bearing wall and partial or complete collapse of the building.

A fundamental assumption in this study is that out-of-plane walls are securely anchored to the floor or roof diaphragms at each level, since this is a simple, low-cost retrofit that greatly reduces the risk of out-of-plane wall collapse. Unanchored walls act as cantilevers about their base and are therefore highly vulnerable to collapse at low levels of seismic excitation. This study focuses on whether the installation of diaphragm-to-wall anchorage alone is sufficient to ensure adequate out-of-plane wall stability, or whether additional wall retrofit is required.

Floor diaphragms in URM buildings commonly consist of timber sheathing supported on timber framing. In smaller buildings, joists typically span directly between load-bearing URM walls, and are either supported on the ledge created by a change in the number of wythes between adjacent stories, or are embedded in cavities created in the walls for this purpose. In larger buildings, joists may be supported by heavier timber or steel members, and by steel columns in large open plan areas. Sheathing arrangements vary, and include either straight sheathing (perpendicular to the joists) or diagonal sheathing (typically at 45° to the joists), applied in either one or two layers. While the in-plane stiffness of such diaphragms varies depending on the configuration, in general the stiffness is very low, and the diaphragm response is dominated by shear deformation.

Under seismic loading in a simple URM building with walls connected to the diaphragms, the inertial forces from the out-of-plane walls are transferred through the floor diaphragms to the in-plane walls, which carry the forces to the foundation. Clearly, the response of the floor diaphragm in such a load resisting system will have a significant influence both on the displacement demands imposed on the out-of-plane walls as well as the loads induced on the in-plane walls. Should stiff, uncracked out-of-plane walls be spanning vertically between floor diaphragms, the response of such a system could be readily modeled using traditional methods. However, the 2-way interaction between cracked out-of-plane walls and flexible floor diaphragms is neither intuitively understood nor easily modeled using traditional methods.

A study currently under way at the University of British Columbia (UBC) intends to address this issue in greater detail through experimental and analytical means. Full-scale shake table tests were carried out on URM wall specimens using a testing apparatus which allows for the simulation of flexible diaphragm boundary conditions. Three wall specimens were successfully tested at the time of writing. This paper describes the setup and preliminary results of the experimental portion of the study, as well as additional work planned.

2. PREVIOUS STUDIES ON OUT-OF-PLANE WALL BEHAVIOUR WITH FLEXIBLE DIAPHRAGMS

Significant previous research on the dynamic out-of-plane response of URM walls began with the tests performed by ABK Joint Venture (1981). In this study, 22 wall specimens with different overburden loads and height to thickness (h/t) ratios were tested under dynamic loading. The ABK dynamic tests were carried out using displacement-controlled actuators at both the top and bottom of the walls. The issue of diaphragm flexibility was addressed by estimating the input motions at the top and bottom of walls using a computer model that consisted of a non-linear shear-deformable beam representing the diaphragm, and lumped masses on the beam representing the out-of-plane walls. The calculated diaphragm response was then applied to the actuators. This test design eliminated the possibility for observing the effects of interaction between out-of-plane wall rocking and diaphragm flexibility. Recommendations from the ABK testing program are reflected in allowable h/t limits specified in ASCE 41 Seismic Rehabilitation Standard (ASCE, 2007). The effects of diaphragm flexibility stemming from the ABK study are implicitly included in the ASCE allowable h/t limits, but no distinction is made in the standard regarding applying the limits to systems with different diaphragm flexibilities.

Cohen (2001) and Simsir (2004) conducted ½-scale shake table testing to investigate the influence of diaphragm flexibility on the performance of reinforced and unreinforced masonry walls, respectively, in one story buildings. Cohen observed that the overall deformation response of low-rise masonry buildings with typical timber diaphragms is dominated by the in-plane response of the diaphragms rather than of the in-plane masonry walls. The wall specimens tested by Simsir were subjected to significant overburden loads to represent lower-storey conditions, which has the effect of increasing the dynamic stability of the cracked wall. In both of these studies, diaphragm flexibility was only simulated at the top of the wall. Meisl et al. (2007) performed full-scale shake table testing of solid clay brick URM walls subjected to out-of-plane excitation, with approximately equal input motions at the top and bottom of the walls. The tests conducted by Meisl simulated rigid diaphragm conditions, in which the top and bottom of the walls were subjected to equal and in-phase displacement demands. The critical condition of upper-storey walls connected to flexible diaphragms has yet to be sufficiently addressed and their stability and safety in future earthquakes remains poorly quantified.

3. EXPERIMENTAL PROGRAM

The following section describes the specimens, apparatus, and protocol of the experimental study.

3.1. Wall Specimens

Three wall specimens were constructed by professional masons in the Earthquake Engineering Research Facility (EERF) at the University of British Columbia (UBC). Brick units were solid and measured 64x89x191mm. The wall specimens were intended to represent a portion of a top-storey wall in an early 1900s load-bearing URM building in British Columbia. Type O mortar (1:2:9 cement:lime:sand) was considered an appropriate representation of existing URM building mortar quality because of its low compressive strength. Brick units were placed dry to further minimize the bond strength. Materials testing results were not available at the time of writing.

Two 3-wythe walls (A & B) and one 2-wythe wall (C) were constructed. Walls A and C represented top-storey walls while wall B represented a wall in a one-storey building. These are the most critical locations for OOP wall failure due to the low overburden load on these walls. The 3-wythe walls measured approximately 1500mm long, 4000mm high, and 290mm thick. The 2-wythe wall measured approximately 1500mm long, 2800mm high, and 190mm thick. American bond was used in all walls with a single header course at every sixth course (Figure 1). Slenderness ratios of the walls ranged between approximately 13.7 and 14.7.

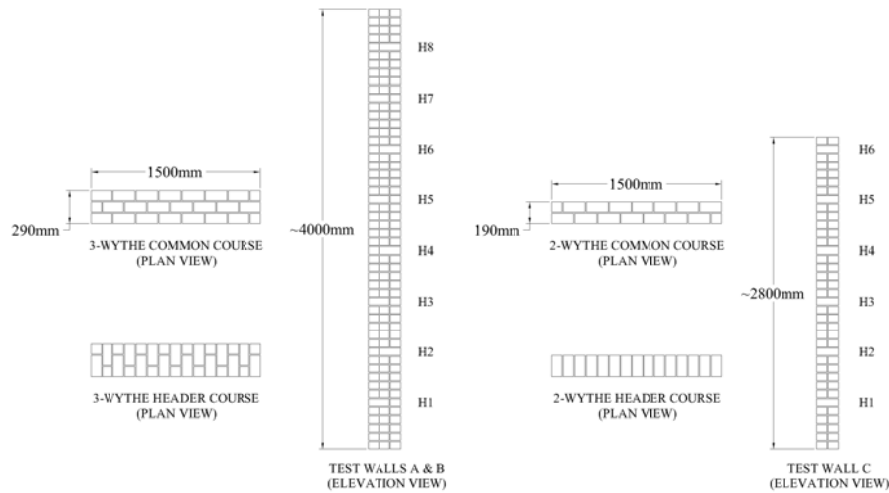


Figure 1. Test wall geometry

3.2. Apparatus

The test apparatus (Figure 2) consists of steel frame components fastened to a uni-axial displacement-controlled shake table. When loaded into the apparatus, the base of each wall specimen is supported on a rolling steel carriage which travels on rails on top of the shake table, in the direction of motion of the shake table. This carriage is connected to the shake table using coil springs, which have been designed to simulate the 1st-mode in-plane response of a flexible floor diaphragm. The periods achieved in the experimental system were approximately 1.7 seconds for walls A and B, and 1.3 seconds for wall C.

A stiff steel braced frame – representing the in-plane walls – of the same height as the test walls is fastened to the shake table. The table motion is transferred to the top of this frame with minimal amplification. The study thus assumes that the flexibility of the in-plane walls is negligible compared to that of the diaphragms. A second rolling steel carriage travels on top of this steel frame, and is connected to the frame with coil springs identical to those at the base. The top of the wall is connected to this carriage, thereby also simulating the response of a flexible diaphragm at the top of the wall. Both the top and bottom carriages can be ‘locked out’ by fastening the carriages rigidly to the steel frame. In this case, the ground motion is applied directly to the wall. For walls A and C, both the top and bottom connections were flexible. For Wall B, the bottom connection was locked out and the top connection was flexible.

A steel plate with a milled vertical slot is fastened underneath the top carriage on each side. A channel is clamped to the top of the wall; a steel pin is fastened to each end of this channel and protrudes past the end of the wall. When assembled, the pins at the top of the wall travel within the vertical slots on the carriage plates, allowing the top of the wall free rotation and vertical displacement.

The walls were constructed on top of wide-flange beam sections to allow them to be lifted into place in the testing apparatus. A strip of ultra-high molecular weight polyethylene (UHMW) was fastened to each side of the wall at the base. A steel bar with a stiff rubber spacer, also lined with a UHMW strip, was fastened to the wide-flange beam and snug-tightened against the wall on each side. The bearing surface between the 2 pieces of UHMW on each side were coated with grease to reduce friction. This connection effectively restrained the lateral displacement of the base of the wall, but allowed the base of the wall to rotate and lift up with minimal resistance.

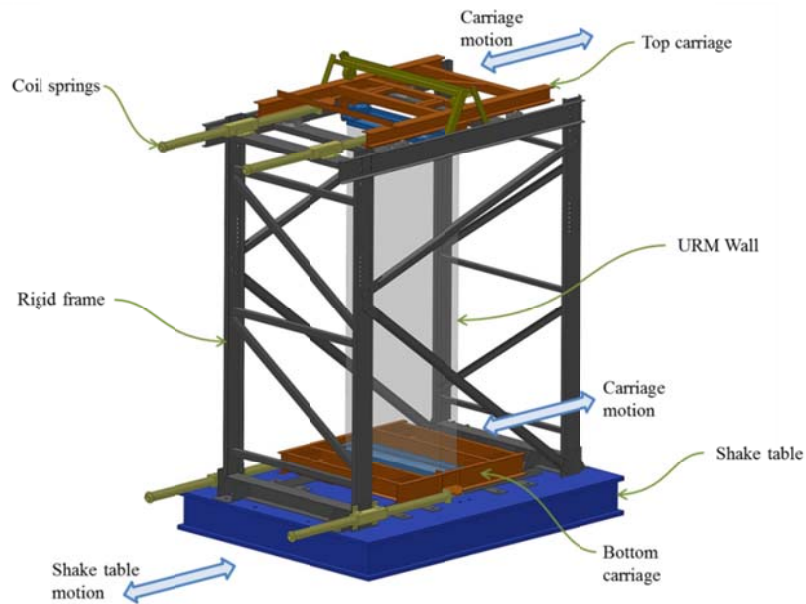


Figure 2. Graphical representation of test apparatus

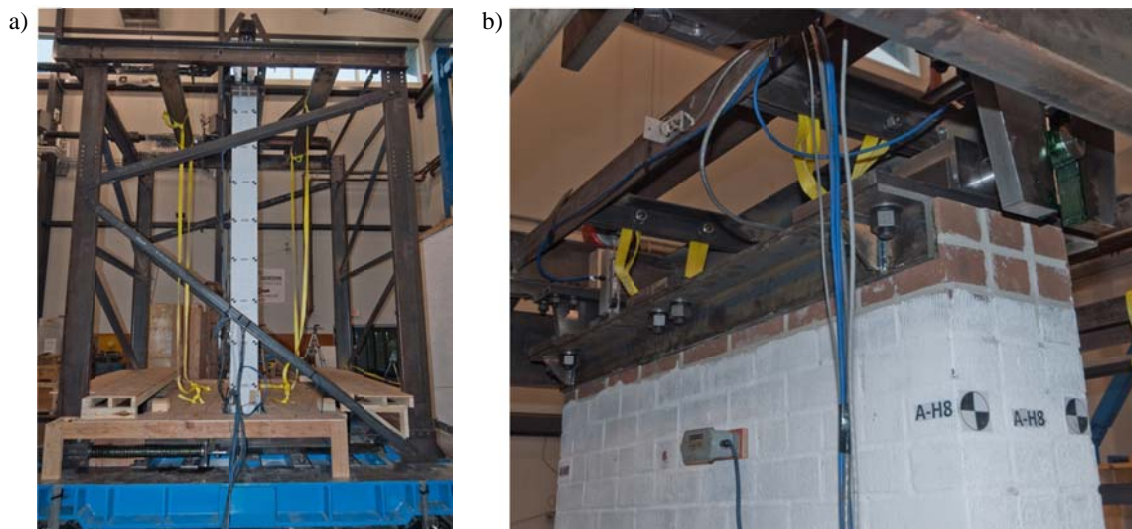


Figure 3. Photos of test apparatus: a) elevation view, b) detail of top connection

The boundary conditions achieved with this test apparatus are idealized representations of the conditions that would be encountered in existing buildings. These conditions were designed to ensure that the test results could be modelled accurately in the analytical portion of the study. Examining the effect of varying boundary conditions (e.g. partial rotational restraint due to wall-diaphragm connections, or arching action in walls due to vertical restraint) was beyond the scope of this study, but could be considered as a separate variable in future research.

Instrumentation used in the tests consisted of accelerometers and displacement transducers. Horizontal acceleration and displacement were measured at each header course on the wall, as well as on the top and bottom carriages, the top of the frame, and the shake table. Vertical displacement of the pins at the top of the wall and the uplift at each side at the base of the wall were measured. Vertical displacement at each end of the shake table was also measured to detect any potential uplift.

3.3. Ground motions

Two ground motions were used as input to the shake table, with one motion selected for significant long-period spectral response and the other for a dominant short-period spectral response. The long-period motion selected was recorded during the 22 February 2011 earthquake in Christchurch, New Zealand. It was recorded at the Christchurch Hospital, and is referred to in this paper as ‘CHHC1’. The short-period motion selected was recorded during the 18 October 1989 earthquake in Loma Prieta, California. It was recorded at the Gavilan College in Gilroy, and is referred to in this paper as ‘NGA0763’. Response spectra and displacement time histories of the two motions as recorded on the shake table are shown in Figures 4 and 5, respectively.

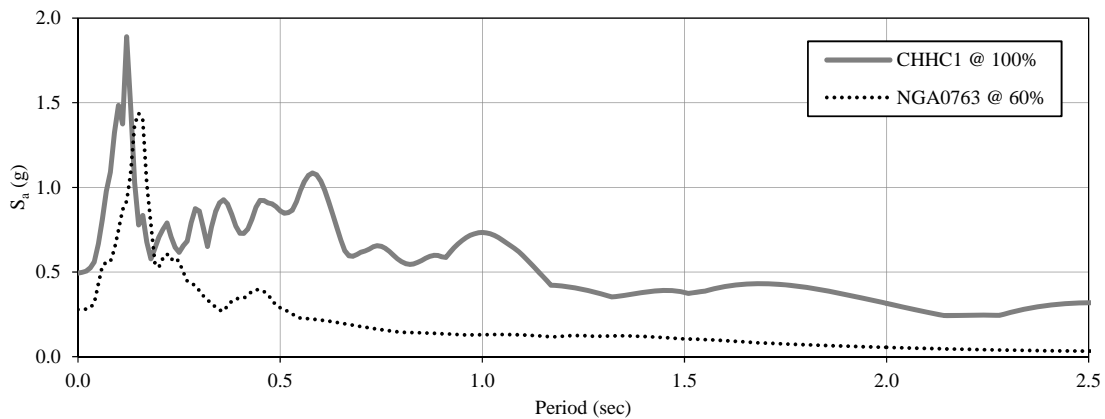


Figure 4. Response spectra of shake table motions

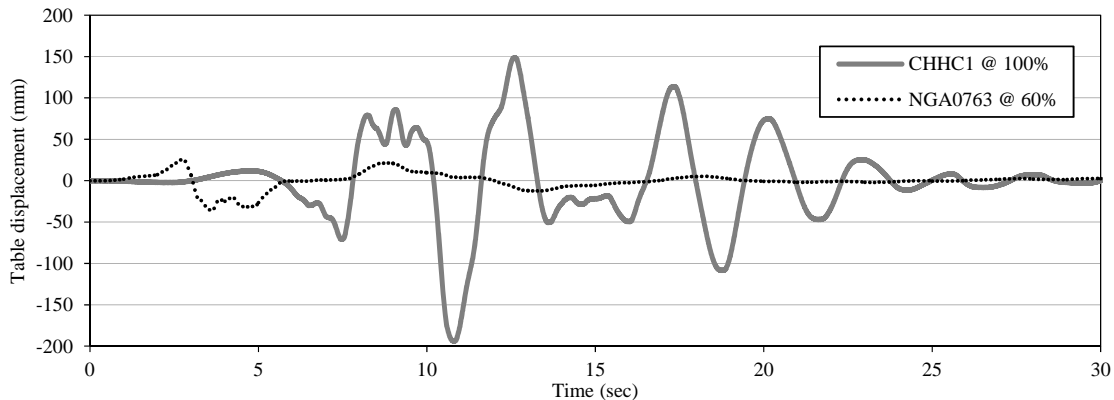


Figure 5. Displacement time histories of shake table motions

Scale factors are shown relative to the original motion as recorded during the earthquake, and reference the magnitude of the displacement time history. It can be observed that the displacement control of the shake table results in significant response amplification at the natural frequency of the hydraulic system, producing a large response peak at a period of about 0.1 to 0.15 seconds. The effect of this amplification was notable for runs in which the carriages were locked out; however, for runs in which the carriages were driven through the springs, this amplification was filtered out due to the much longer natural period of the spring-carriage-wall system.

3.4. Test protocol

The mortar used in the construction of the test walls (Type O) is of significantly lower strength than that used in modern structural masonry. However, in particular the flexural bond strength of walls found in early 1900s buildings may be weaker still than that of the test walls. To produce accelerations in the test walls sufficient to initiate cracking while the carriages were driven through the springs would have required a large scale factor on the CHHC1 run (>100%). Applying such a large ground motion to an uncracked wall would likely have caused collapse in the same run that initiated cracking, which would have precluded the observation of the response of the cracked wall. It was therefore decided not to rely on the cracking resistance of the test walls in assessing their dynamic stability on the shake table, but rather to ‘assume’ that the walls would experience cracking at very low levels of excitation. The test protocol thus consisted of three stages: (1) uncracked wall, carriages driven through springs, CHHC1 motion at several magnitudes, (2) uncracked wall, carriages locked out, NGA0763 motion, ramped up until cracking initiated, and (3) cracked wall, carriages driven through springs, CHHC1 motion, ramped up until collapse. For each wall, the motions run and the state of the carriages are shown in Table 1.

Table 1. Test protocol

Stage	Motion	Wall A			Wall B			Wall C		
		Scale	Carriages		Scale	Carriages		Scale	Carriages	
			Top	Bottom		Top	Bottom		Top	Bottom
1	CHHC1	10%	Flexible	Flexible	50%	Flexible	Locked	50%	Flexible	Flexible
		30%			70%			80%		
		50%			70%			80%		
		70%			70%			80%		
		80%			70%			80%		
		100%			70%			80%		
2	NGA0763	50%	Locked	Locked	60%	Locked	Locked	60%	Locked	Locked
		60%			70%			70%		
3	CHHC1	30%	Flexible	Flexible	50%	Flexible	Locked	50%	Flexible	Flexible
		50%			70%			70%		
		70%			80%			80%		
		80%			90%			90%		
		100%			100%			100%		
		110%			110%			110%		
		120%			120%			120%		

4. RESULTS OF DYNAMIC TESTING

Preliminary results from dynamic tests of walls A, B, and C are presented in the following section.

4.1. Rigid diaphragm response

Typical acceleration profiles along the height of the wall, including at the top and bottom carriages, are shown in Figure 6 for uncracked and cracked conditions during the fixed-carriage runs for Wall A.

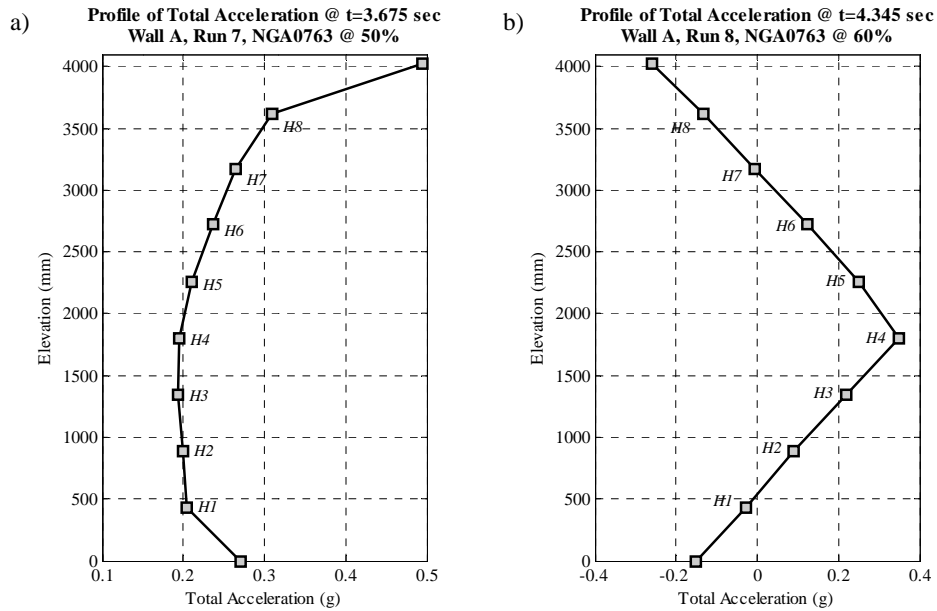


Figure 6. Typical (a) uncracked and (b) cracked acceleration profiles

Prior to undergoing significant rigid-body rocking, cracks were visually nearly imperceptible. In each wall, a single horizontal crack occurred near mid-height. In every case, the crack occurred at a header course, and at the brick-mortar interface. Wall A sustained a horizontal crack along the top of header course 4, Wall B along the bottom of header course 5, and Wall C along the top of header course 3. In the case of Wall C, the crack stepped down by 1 brick at one end of the wall. Even after sustained rocking in later runs, all cracks consistently closed up without any horizontal offset and with minimal spalling of mortar. A typical crack after significant rocking has occurred is shown in Figure 7; the crack was marked in felt pen after the run in which it initiated to improve its visibility.



Figure 7. Crack in Wall C

4.2. Flexible diaphragm response

Time histories of Walls A, B, and C for flexible-diaphragm runs at 100% scale are shown in Figure 8. In this figure, the table displacement is shown relative to a fixed external reference, while the carriage and wall displacements are shown relative to the table (i.e. when these lines are flat, the movement of the wall or carriage is in unison with the table).

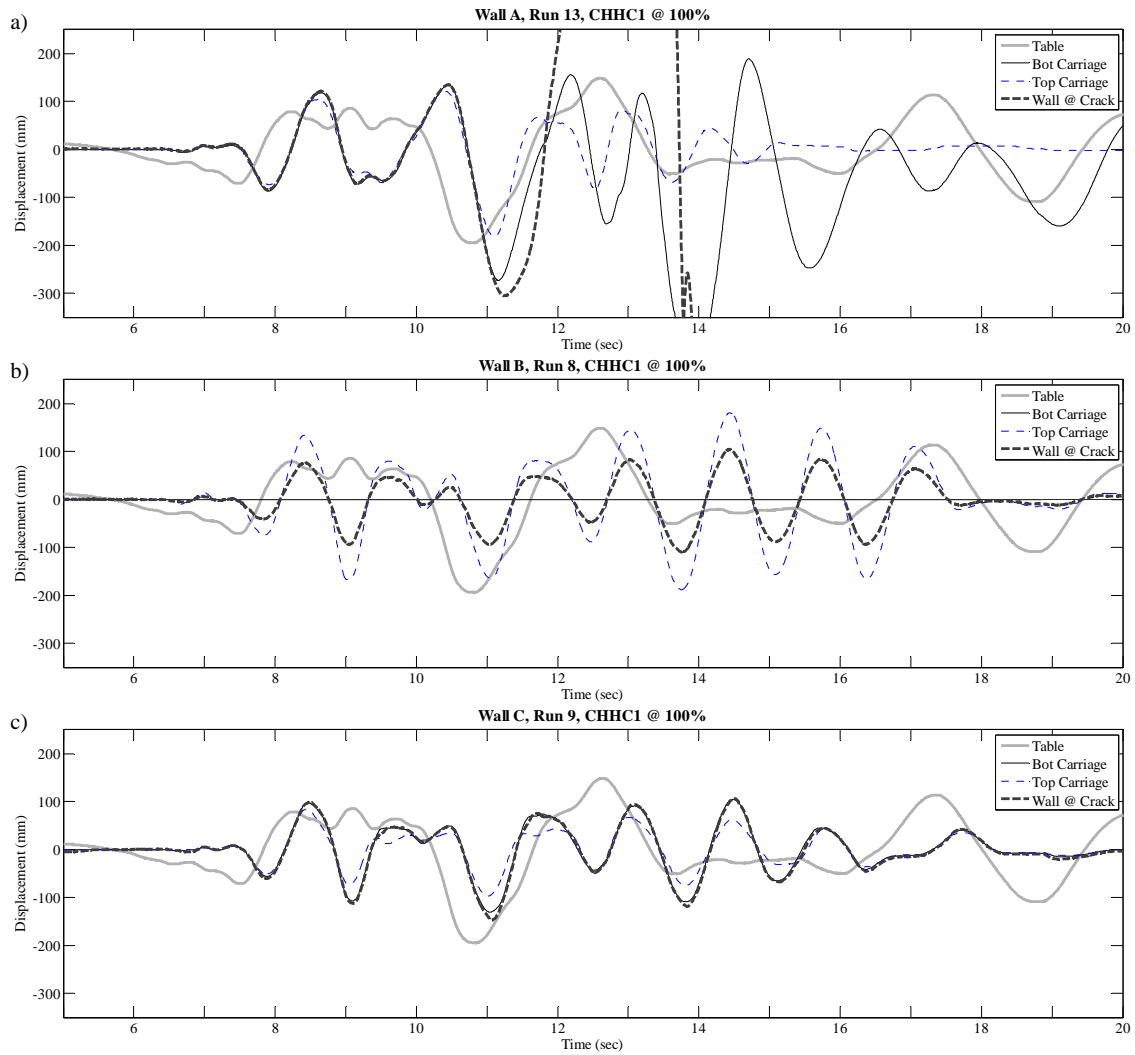


Figure 8. Flexible diaphragm response time histories

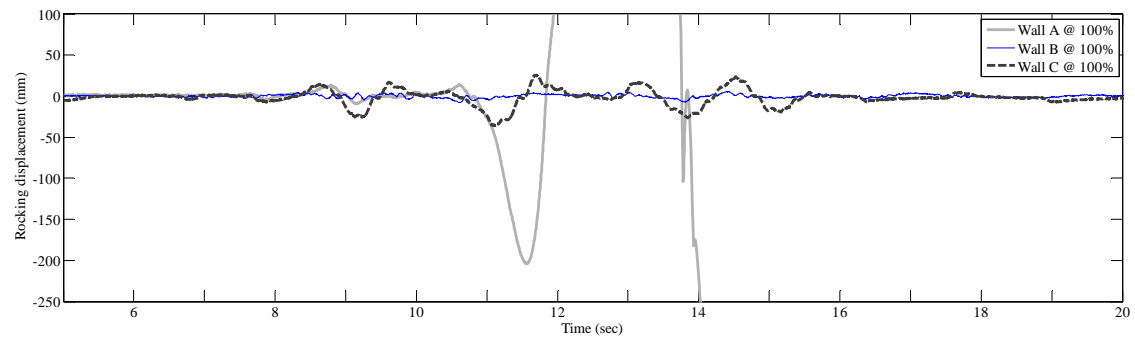


Figure 9. Flexible diaphragm rocking displacement time histories

Wall A collapsed at the 100% level of excitation, whereas Walls B and C remained stable. Both collapsed at 120%, two runs later. For each wall, the maximum carriage displacements reached during runs in which the cracked wall remained stable are shown in Table 2.

Table 2. Peak carriage displacements in stable runs

Wall	Peak carriage displacement (mm)	
	Bottom	Top
A	180	157
B	0	206
C	142	102

The rocking displacement shown in Figure 9 is defined as the difference between the measured displacement of the wall at the crack height and the straight-line interpolation between the top and bottom of the wall at the same height. In Figure 10, the peak rocking displacement from each run is shown relative to the magnitude of the ground motion in that run, with the rocking displacement normalized to the wall thickness. The static instability limit can be defined as the point when the normalized rocking displacement is equal to 1.

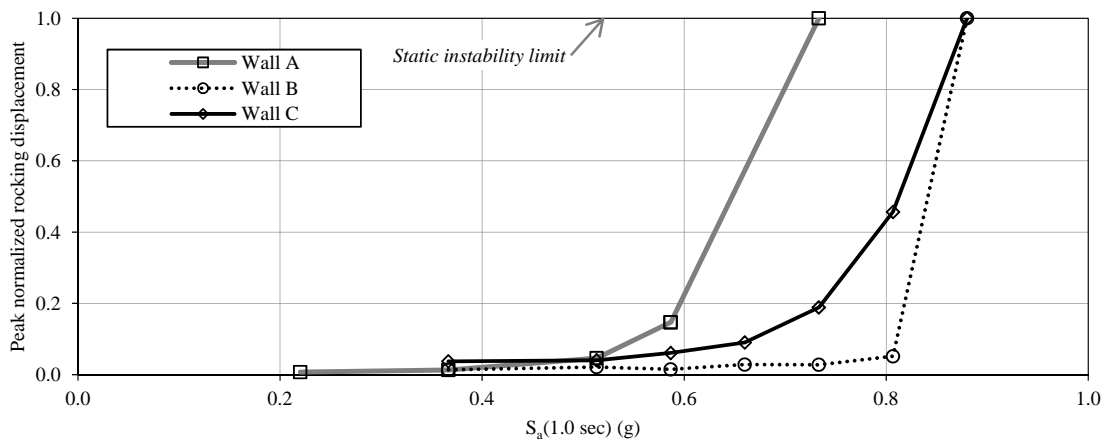


Figure 10. Peak normalized rocking displacement vs. magnitude of ground motion

Walls which were connected to flexible supports at both the top and bottom (A and C) exhibited significant rocking displacement in runs prior to the collapse run. In contrast, Wall B, which was connected to a fixed base and a flexible top support, exhibited very limited rocking in all runs prior to the collapse run. This is a notable difference from the observations of Meisl et al. (2007).

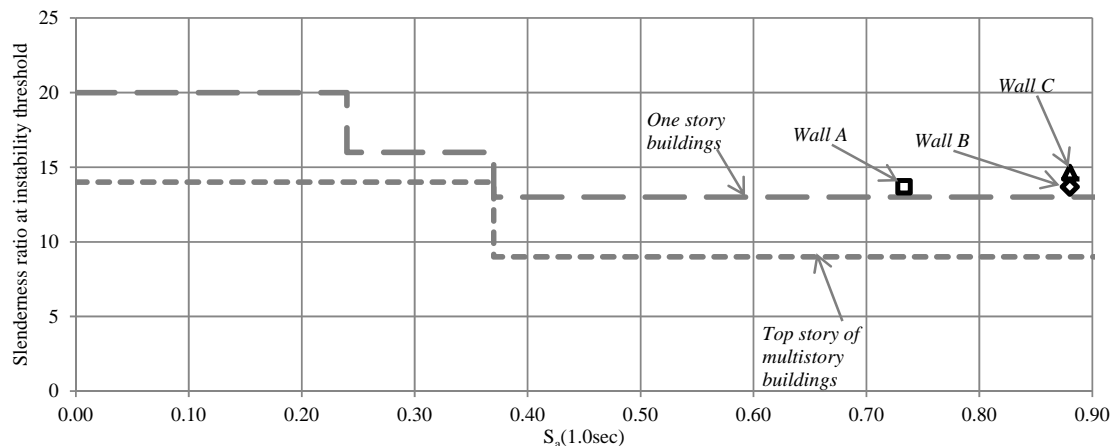


Figure 11. ASCE 41 stability limits & experimental collapse observations

In Figure 11, the observed collapse points and wall slenderness ratios of the test specimens are shown on a plot of the allowable slenderness ratios stipulated for out-of-plane URM walls in ASCE 41. At present, the allowable slenderness ratios are independent of diaphragm flexibility, and are specified as a function of $S_a(1.0\text{sec})$. For consistency, the spectral acceleration of the applied ground motions in the test were also plotted at a period of 1.0 second, despite this not being the natural period of the wall-spring-carriage system in the tests. The authors intend to examine the effect of evaluating wall stability with respect to this natural diaphragm period in the upcoming analytical portion of the study.

4. CONCLUSIONS AND UPCOMING WORK

While it is too early in the study to reach definite conclusions, the preliminary results suggest that ASCE41 limits may be conservative with respect to assessing wall stability connected to flexible diaphragms. The authors intend to evaluate this suggestion comprehensively by carrying out a parametric study using a rigid-body rocking model previously developed by Sharif et al. (2007) and expanded by Penner et al. (2011).

The second phase of the experimental study will consist of shake table testing of retrofitted URM wall specimens. Two additional specimens of the same size as walls A and B were constructed in April 2012 for this purpose. Potential retrofits under consideration include steel strong-backs, near-surface mounted CFRP, FRP wrap, and/or a combination of these systems. This phase of the study will aim to identify retrofit solutions that are as economical and aesthetically unobtrusive as possible while providing collapse-prevention performance in historic buildings in areas of high seismic hazard.

ACKNOWLEDGEMENT

The authors acknowledge the support of the Natural Sciences and Engineering Research Council of Canada, the Canadian Seismic Research Network, and the staff members of the Civil Engineering Department at UBC.

REFERENCES

- ABK Joint Venture. (1981). Methodology for Mitigation of Seismic Hazards in Existing Unreinforced Masonry Buildings: Wall Testing, Out-Of-Plane. ABK Topical Report 04.
- ASCE. (2007). Seismic Rehabilitation of Existing Buildings, ASCE/SEI 41/06, American Society of Civil Engineers, Reston, Virginia.
- Cohen, G. L. (2001). Seismic Response of Low-Rise Masonry Buildings with Flexible Roof Diaphragms. Master's Thesis, University of Texas at Austin.
- Simsir, C. (2004). Influence of Diaphragm Flexibility on the Out-of-Plane Dynamic Response of Unreinforced Masonry Walls. Ph.D. Thesis, University of Illinois at Urbana-Champaign.
- Meisl, C., Elwood, K.J., and Ventura, C.E. (2007). Shake table tests on the out-of-plane response of unreinforced masonry walls. *Canadian Journal of Civil Engineering* **34:11**, 1381-1392.
- Oliver, S. J. (2010). A Design Methodology For The Assessment and Retrofit Of Flexible Diaphragms In Unreinforced Masonry Buildings. *SESOC Journal* **23:1**.
- Penner, O. and Elwood, K.J. (2011). Effect of Diaphragm Flexibility on Seismic Vulnerability of Out-Of-Plane Unreinforced Masonry Walls Subjected to Ground Motions from the 2010 Darfield Earthquake. 9th Australasian Masonry Conference, Queenstown, New Zealand, 15-18 February.
- Sharif, I., Meisl, C., and Elwood, K.J. (2007). Assessment of ASCE 41 Height-to-Thickness Ratio Limits for URM Walls. *Earthquake Spectra* **23:4**, 893-908.